

# Phase-dependent fluctuations of intermittent resonance fluorescence

Héctor M. Castro-Beltrán,<sup>1,2,\*</sup> Ricardo Román-Ancheyta,<sup>2,†</sup> and Luis Gutiérrez<sup>1,‡</sup>

<sup>1</sup>*Centro de Investigación en Ingeniería y Ciencias Aplicadas, Universidad Autónoma del Estado de Morelos, Avenida Universidad 1001, 62209 Cuernavaca, Morelos, México*

<sup>2</sup>*Instituto de Ciencias Físicas, Universidad Nacional Autónoma de México, Apartado Postal 48-3, 62251 Cuernavaca, Morelos, México*

(Dated: December 4, 2015)

Electron shelving gives rise to bright and dark periods in the resonance fluorescence of a three-level atom. The corresponding incoherent spectrum contains a very narrow inelastic peak on top of a two-level-like spectrum. Using the theories of balanced and conditional homodyne detection we study ensemble averaged phase-dependent fluctuations of intermittent resonance fluorescence. The sharp peak is found only in the spectra of the squeezed quadrature. In balanced homodyne detection that peak is positive, which greatly reduces the squeezing, also seen in its variance. In conditional homodyne detection CHD, for weak to moderate laser intensity, the peak is negative, enhancing the squeezing, and for strong fields the sidebands become dispersive which, together with the positive sharp peak dominate the spectrum. The latter effect is due to non-negligible third order fluctuations produced by the atom-laser nonlinearity and the increased steady state population of the shelving state. A simple mathematical approach allows us to obtain accurate analytical results.

PACS numbers: 42.50.Lc, 42.50.Ct, 42.50.Hz

## I. INTRODUCTION

A photon emitter with peculiar fluctuations is a single three-level atom with a laser-driven strong transition competing with a coherently or incoherently driven weak transition. The occasional population of a long-lived state, an effect called electron shelving, thus produces intermittence (blinking) in the resonance fluorescence of the strong transition. Photon statistics of the fluorescence have been thoroughly studied for three-level atomic systems [1], in which case the process is ergodic, i.e., when the mean bright and dark periods are finite. For a single quantum dot or molecule the statistics are more complicated if the process is not ergodic [2]. In the spectral domain, ergodic shelving manifests in the appearance of a very narrow inelastic peak on top of the central peak of the two-level-like spectrum. This has been well studied analytically and numerically [3–5] and observed experimentally [6]. In the latter, heterodyne detection was used, which allows for very high spectral resolution [7]. In their paper [6], Bühner and Tamm suggest performing complementary phase-dependent measurements of the fluorescence; so far, there are no reports yet, perhaps due to experimental restrictions.

Squeezing, the reduction of fluctuations below those of a coherent state in a quadrature at the expense of the other, is weak in resonance fluorescence [8, 9]. The low collection and imperfect quantum efficiency of photodetectors have been the main barriers for the observation of squeezing, though recent experimental progress tackle

these issues. On the one hand, there is the increased solid angle of emission captured with minimal disturbance of the photon density of states surrounding the atom [10]. On the other is the development of conditional detection schemes based on homodyne detection that cancel the finite quantum efficiency issue [11–18]. We discuss two of them.

Homodyne correlation measurement (HCM), proposed by Vogel [11, 12] (see also [19]), consists of intensity correlations of the previously mixed source and weak local oscillator fields, thus canceling the detector efficiency factors. The output contains several terms, including the variance and an amplitude-intensity correlation. Very recently, HCM was used to observe squeezing in the resonance fluorescence of a single two-level quantum dot [20] in conditions close to those for free-space atomic resonance fluorescence. In fact, in the first demonstration of HCM the amplitude-intensity correlation of the fluorescence of a single three-level ion in the  $\Lambda$  configuration was observed [21] though not yet in the squeezing regime.

Conditional homodyne detection (CHD) was proposed and demonstrated by Carmichael, Orozco and coworkers [13, 14]. This consists of balanced homodyne detection (BHD) of a quadrature conditioned on an intensity measurement of part of the emitted field; it gives the amplitude-intensity correlation of HCM but measured directly, without the interfering terms. As in the intensity correlations, the conditioning cancels the dependence on detector efficiency. The intensity detection channel has nontrivial effects on the quadrature signals. The amplitude-intensity correlation is of third order in the field amplitude, hence it allows for third order fluctuations. Initially, CHD was devised for weak light emitters, neglecting the third order fluctuations. This allowed to identify the Fourier transform of the correlation as the spectrum of squeezing [13, 14]. However, recent work on

\*Electronic address: hcastro@uaem.mx

†Electronic address: ancheyta6@gmail.com

‡Electronic address: luis.gutierrez@uaem.mx

CHD of two-level atom resonance fluorescence has shown important deviations from the spectrum of squeezing due to increasing nonlinearity in the atom-laser interaction [22, 23]. An additional display of these non-Gaussian fluctuations is found in the asymmetry of the correlation in cavity QED [24] and in the resonance fluorescence of a  $V$ -type three-level atom [25–27] and of two blockading Rydberg atoms [28].

In this paper we investigate theoretically ensemble-averaged phase-dependent fluctuations of the intermittent (ergodic) resonance fluorescence of a single three-level atom (3LA). Besides numerical solutions for the one- and two-time expectation values, we obtain approximate analytical solutions which are very accurate in the limit when the decay rate of the strong transition is much larger than those of the weak transitions. Our solutions are simple and reflect clearly the time and spectral scales. Thus we begin by writing the expression for the coherent and phase-independent incoherent spectra of the 3LA, studied numerically at length in Ref. [5].

We compare the spectra and variances of an ideal BHD approach, as it could also be obtained from HCM, with those of the CHD method. They have in common that the sharp extra peak [3–6], on atom-laser resonance, is a feature *only* of the quadrature that features squeezing; in the other quadrature the spectrum is a simple broad positive Lorentzian. In the weak field limit, while both methods give similar spectra for a two-level atom (2LA), the sharp peak has opposite sign, reducing the squeezing in BHD and enhancing the negative peak in CHD. For strong laser field the third order fluctuations of CHD distort the positive Lorentzian sidebands of the Mollow triplet and turn them dispersive for both 2LA and 3LA. However, for the 3LA, both the sharp peak and the dispersive sidebands are much larger than the second order spectrum.

This paper is organized as follows: In Sec. II we introduce the atom-laser model and obtain approximate analytic results. In Sec. III we calculate the phase-independent spectrum, and in Sec. IV the phase-dependent spectra and variances. Sections V and VI are devoted to the amplitude-intensity correlation by CHD and its associated spectra, respectively. Finally, conclusions are given in Sec. VII. Two appendices summarize the analytic and numerical methods employed.

## II. ATOM-LASER MODEL AND SOLUTIONS

We consider a single three-level atom where a laser of Rabi frequency  $\Omega$  drives a transition between the ground state  $|g\rangle$  and an excited state  $|e\rangle$ . The excited state has two spontaneous emission channels: one directly to the ground state with rate  $\gamma$  for the driven transition, and one via a long-lived shelving state  $|a\rangle$  with rate  $\gamma_d$ , which in turn decays to the ground state with rate  $\gamma_a$  (see Fig. 1). In the limit

$$\gamma \gg \gamma_d, \gamma_a \quad (1)$$

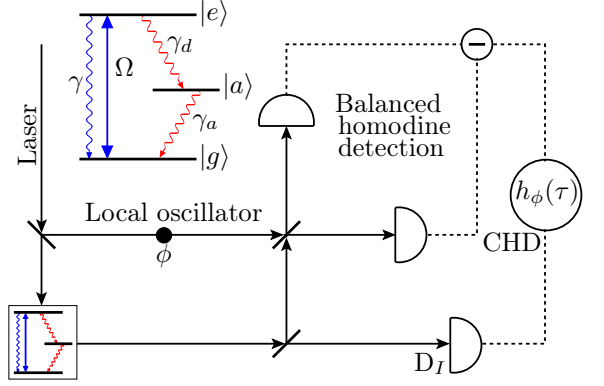


FIG. 1: (Color online) Scheme of conditional homodyne detection (CHD). Blocking the path to the lower detector,  $D_I$ , realizes the standard balanced homodyne detection (BHD). The inset shows the three-level atom-laser interaction and spontaneous decays.

the fluorescence of the driven transition features well defined bright and dark periods of average lengths

$$T_B = \frac{2\Omega^2 + \gamma^2}{\gamma_d\Omega^2}, \quad T_D = \gamma_a^{-1}, \quad (2)$$

respectively, as calculated in Ref. [5] using a random telegraph model.

Throughout this paper we assume zero atom-laser detuning. This serves two purposes: first, we limit to the essentials of the main topics; second, with further assumptions discussed later, we obtain close approximate analytical solutions. The master equation for the atomic density operator, in the frame rotating at the laser frequency, can be written as

$$\begin{aligned} \dot{\rho}(t) = & -i\frac{\Omega}{2}[\sigma_{eg} + \sigma_{ge}, \rho] \\ & + \frac{\gamma}{2}(2\sigma_{ge}\rho\sigma_{eg} - \sigma_{ee}\rho - \rho\sigma_{ee}), \\ & + \frac{\gamma_d}{2}(2\sigma_{ae}\rho\sigma_{ea} - \sigma_{ee}\rho - \rho\sigma_{ee}), \\ & + \frac{\gamma_a}{2}(2\sigma_{ga}\rho\sigma_{ag} - \sigma_{aa}\rho - \rho\sigma_{aa}), \end{aligned} \quad (3)$$

where  $\sigma_{jk} = |j\rangle\langle k|$  are atomic projector operators which obey the inner product prescription  $\langle j|k\rangle = \delta_{jk}$ .

We obtain two sets of equations. The first one is:

$$\dot{\rho} = \mathbf{M}\rho + \mathbf{b}, \quad (4a)$$

where  $\rho = (\rho_{eg}, \rho_{ge}, \rho_{ee}, \rho_{gg})^T$ ,  $\mathbf{b} = (0, 0, 0, \gamma_a)^T$ , and

$$\mathbf{M} = \begin{pmatrix} -\gamma_+/2 & 0 & i\Omega/2 & -i\Omega/2 \\ 0 & -\gamma_+/2 & -i\Omega/2 & i\Omega/2 \\ i\Omega/2 & -i\Omega/2 & -\gamma_+ & 0 \\ -i\Omega/2 & i\Omega/2 & \gamma_- & -\gamma_a \end{pmatrix}, \quad (4b)$$

where

$$\gamma_+ = \gamma + \gamma_d, \quad \gamma_- = \gamma - \gamma_a. \quad (5)$$

Here we have eliminated the population  $\rho_{aa}$  due to conservation of probability,  $\rho_{gg} + \rho_{ee} + \rho_{aa} = 1$ .

The other set involves the coherences linking the states  $|e\rangle$  and  $|g\rangle$  to the state  $|a\rangle$ , i.e.,  $(\rho_{ga}, \rho_{ag}, \rho_{ea}, \rho_{ae})^T$ . They evolve with damped oscillations with zero mean. The two sets are decoupled, and only the first one is relevant for the purposes of this work.

We obtain first the steady state of the density operator (labeled with the abbreviation *st*). For a more compact notation we define  $\alpha_- = \rho_{eg}^{st} = \langle \sigma_- \rangle_{st}$ ,  $\alpha_+ = \alpha_-^*$ , and  $\alpha_{jj} = \rho_{jj}^{st} = \langle \sigma_{jj} \rangle_{st}$ . We have

$$\alpha_{\mp} = \mp i \frac{Y/\sqrt{2}}{1 + Y^2 + (q/2)Y^2}, \quad (6a)$$

$$\alpha_{ee} = \frac{Y^2/2}{1 + Y^2 + (q/2)Y^2}, \quad (6b)$$

$$\alpha_{gg} = \frac{1 + Y^2/2}{1 + Y^2 + (q/2)Y^2}, \quad (6c)$$

$$\alpha_{aa} = q\alpha_{ee}, \quad (6d)$$

where

$$q = \gamma_d/\gamma_a, \quad Y = \sqrt{2}\Omega/\gamma_+. \quad (7)$$

For  $\gamma_d = 0$  ( $q = 0$ ) we recover the results of the 2LA.

Equations (4a) are still too complicated to be solved analytically in the general case. However, in the limit (1), very good approximate solutions are obtained (see Appendix A for more details). We use a Laplace transform approach to obtain approximate expectation values of the atomic vector,  $\mathbf{s} = (\sigma_-, \sigma_+, \sigma_{ee}, \sigma_{gg})^T$ , and two-time correlations. With the atom initially in its ground state,  $\langle \mathbf{s}(0) \rangle = (0, 0, 0, 1)^T$ , the expectation values of the atomic operators are

$$\begin{aligned} \langle \sigma_{\mp}(t) \rangle &= \mp i \frac{Y/\sqrt{2}}{1 + Y^2} f(t) \mp i \frac{\sqrt{2}\gamma_+ Y}{8\delta} (e^{\lambda_+ t} - e^{\lambda_- t}) \\ &\quad + \alpha_{\mp} (1 - e^{\lambda_2 t}), \end{aligned} \quad (8a)$$

$$\langle \sigma_{ee}(t) \rangle = \frac{Y^2/2}{1 + Y^2} f(t) + \alpha_{ee} (1 - e^{\lambda_2 t}), \quad (8b)$$

$$\langle \sigma_{gg}(t) \rangle = e^{\lambda_2 t} - \frac{Y^2/2}{1 + Y^2} f(t) + \alpha_{gg} (1 - e^{\lambda_2 t}), \quad (8c)$$

where

$$\begin{aligned} f(t) &= e^{\lambda_2 t} - \frac{1}{2} \left[ \left( 1 + \frac{3\gamma_+}{4\delta} \right) e^{\lambda_+ t} \right. \\ &\quad \left. + \left( 1 - \frac{3\gamma_+}{4\delta} \right) e^{\lambda_- t} \right], \end{aligned} \quad (9)$$

$$\lambda_1 = -\gamma_+/2, \quad (10a)$$

$$\lambda_2 = -\gamma_a \left( 1 + q \frac{\Omega^2}{2\Omega^2 + \gamma^2} \right), \quad (10b)$$

$$\lambda_{\pm} = -\frac{3\gamma_+}{4} \pm \delta, \quad (10c)$$

and

$$\delta = (\gamma_+/4)\sqrt{1 - 8Y^2}. \quad (11)$$

This approach allows us to identify Eqs. (10) as the eigenvalues of the matrix of coefficients of the master equation (4a). This is much more convenient than attempting to simplify the exact ones, very cumbersome to be reproduced here. The eigenvalues contain the kernel of the atomic evolution, that is, the scales of decay and coherent evolution, as well as the corresponding widths and positions of the spectral components.

The first eigenvalue,  $\lambda_1$ , is exact and gives half the total decay rate from the excited state. Though absent in Eqs. (8), it occurs in the second order correlations (see below). Then,  $\lambda_2$  represents the slow decay rate due to shelving. This makes the steady state to be reached in a long time scale,  $t \sim \gamma_d^{-1}$ . Borrowing from the random telegraph model [5], it is given by  $\lambda_2 = -(T_D^{-1} + T_B^{-1})$ . The two remaining eigenvalues represent the damped coherent evolution; they are real if  $8Y^2 \leq 1$  and complex if  $8Y^2 > 1$ . Eigenvalues  $\lambda_1, \lambda_{\pm}$  contain the two-level-like evolution towards a quasi-steady state (with the decay rate  $\gamma$  of the two-level case replaced by  $\gamma_+$  for the 3LA) that is followed by the slow decay.

The two-time correlations  $\langle \sigma_+(0)\mathbf{s}(\tau)\sigma_-(0) \rangle_{st}$ , which have the initial conditions  $(0, 0, 0, \alpha_{ee})^T$ , are approached as those for  $\langle \mathbf{s}(t) \rangle$ . Using the quantum regression formula (see, e.g., [29]) and  $\mathbf{s}(0) = (0, 0, 0, 1)^T$ , we have

$$\langle \sigma_+(0)\mathbf{s}(\tau)\sigma_-(0) \rangle_{st} = \alpha_{ee} \langle \mathbf{s}(\tau) \rangle_{\mathbf{s}(0)}, \quad (12)$$

i.e., these correlations are identical to Eqs. (8) times the factor  $\alpha_{ee}$  and replacing  $t$  by  $\tau$ .

The approximate analytic solutions to the correlations  $\langle \sigma_+(0)\mathbf{s}(\tau) \rangle_{st}$ , which have the initial conditions  $(\alpha_{ee}, 0, 0, \alpha_+)^T$ , can be similarly obtained (see Appendix A). We use them, though, to obtain the solutions for correlations of fluctuations,  $\langle \Delta\sigma_+(0)\Delta\mathbf{s}(\tau) \rangle_{st}$ , where

$$\Delta\sigma_{jk}(t) = \sigma_{jk}(t) - \langle \sigma_{jk} \rangle_{st}, \quad \langle \Delta\sigma_{jk}(t) \rangle = 0. \quad (13)$$

Hence

$$\langle \Delta\sigma_+(0)\Delta\sigma_{\mp}(\tau) \rangle_{st} = \langle \sigma_+(0)\sigma_{\mp}(\tau) \rangle_{st} - \langle \sigma_+ \rangle_{st} \langle \sigma_{\mp} \rangle_{st}, \quad (14)$$

yielding

$$\begin{aligned} \langle \Delta\sigma_+(0)\Delta\sigma_{\mp}(\tau) \rangle_{st} &= C_1 e^{\lambda_1 \tau} \mp C_+ e^{\lambda_+ \tau} \\ &\quad \mp C_- e^{\lambda_- \tau} \pm C_2 e^{\lambda_2 \tau}, \end{aligned} \quad (15)$$

where

$$C_1 = \frac{1}{4} \frac{Y^2}{1 + Y^2 + (q/2)Y^2}, \quad (16a)$$

$$C_2 = \frac{q}{4} \frac{Y^4}{(1 + Y^2)(1 + Y^2 + (q/2)Y^2)^2}, \quad (16b)$$

$$C_{\mp} = \frac{1}{8} \frac{Y^2[1 - Y^2 \pm (1 - 5Y^2)(\gamma_+/4\delta)]}{(1 + Y^2)(1 + Y^2 + (q/2)Y^2)}. \quad (16c)$$

### III. STATIONARY POWER SPECTRUM

The stationary (Wiener-Khintchine) power spectrum is given by the Fourier transform of the dipole field auto-correlation function,

$$S(\omega) = \frac{1}{\pi\alpha_{ee}} \text{Re} \int_0^\infty d\tau e^{-i\omega\tau} \langle \sigma_+(0) \sigma_-(\tau) \rangle_{st}. \quad (17)$$

The splitting (14) separates the spectrum in two parts:

$$S(\omega) = S_{coh}(\omega) + S_{inc}(\omega), \quad (18)$$

where

$$S_{coh}(\omega) = \frac{|\alpha_+|^2}{\pi\alpha_{ee}} \text{Re} \int_0^\infty e^{-i\omega\tau} d\tau = \frac{|\alpha_+|^2}{\pi\alpha_{ee}} \delta(\omega) \quad (19)$$

and

$$S_{inc}(\omega) = \frac{1}{\pi\alpha_{ee}} \text{Re} \int_0^\infty d\tau e^{-i\omega\tau} \langle \Delta\sigma_+(0) \Delta\sigma_-(\tau) \rangle_{st} \quad (20)$$

are, respectively, the coherent spectrum, due to elastic scattering, and the incoherent (inelastic) spectrum, due to atomic fluctuations.

The main features of the spectrum of the atom-laser system of the previous Section were studied in [5]. The incoherent spectrum consists of a two-level-like structure that becomes a triplet for strong excitation [30], plus a sharp peak, associated to the eigenvalue  $\lambda_2$ , due to the shelving of electronic population in the long-lived state. This three-level system contains the essential physics of the more complex atomic system used for the experimental observation of the sharp peak [6] by heterodyne detection, able to resolve Hz or sub-Hz features [7]. The sharp peak had been predicted for the V and  $\Lambda$  3LA [3, 4], which also feature electron shelving. In Ref. [5] the coherent spectrum of the 3LA was found to be smaller than that of the 2LA (where  $\gamma_d = 0$  and  $q = 0$ ):

$$S_{coh}(\omega) = \frac{1}{\pi(1 + Y^2 + (q/2)Y^2)} \delta(\omega). \quad (21)$$

The difference was found in the incoherent spectrum as the cited narrow extra peak of width  $\Gamma_{ep} = T_D^{-1} + T_B^{-1} = -\lambda_2$ .

Our Laplace transform approach allowed us to obtain a very good analytic approximation to the full spectrum, split into its various components, with their widths and amplitudes readily spotted. Substituting Eqs. (15), (16) and (6a) into Eq. (20) the incoherent spectrum is

$$S_{inc}(\omega) = \frac{1}{\pi\alpha_{ee}} \left[ -C_1 \frac{\lambda_1}{\omega^2 + \lambda_1^2} - C_2 \frac{\lambda_2}{\omega^2 + \lambda_2^2} + C_+ \frac{\lambda_+}{\omega^2 + \lambda_+^2} + C_- \frac{\lambda_-}{\omega^2 + \lambda_-^2} \right]. \quad (22)$$

In Fig. 2 we plot this spectrum with eigenvalues (10) along the exact and 2LA spectra. It reproduces remarkably well the exact spectrum, with the sharp peak being

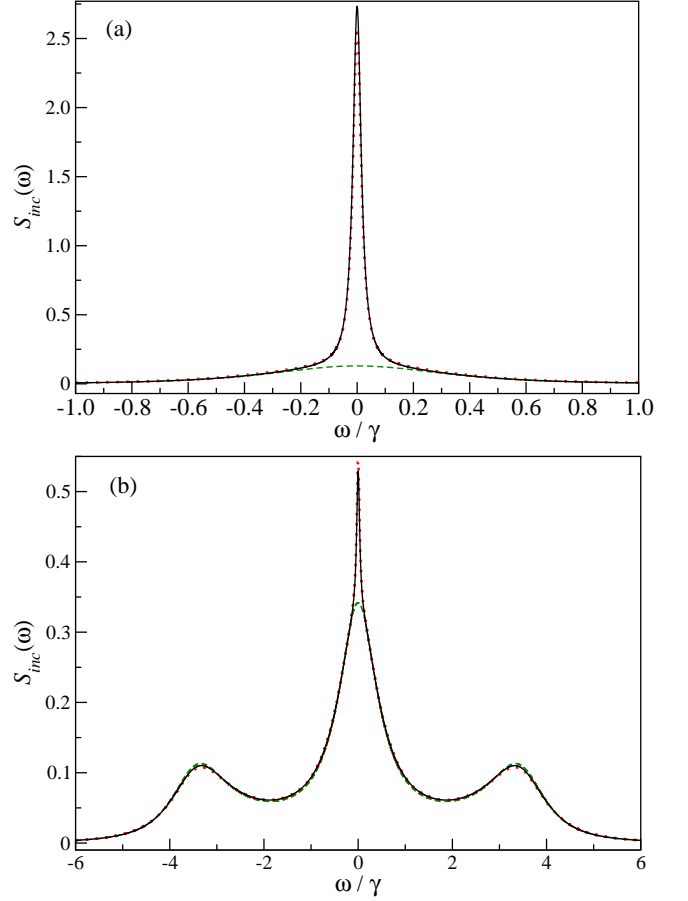


FIG. 2: (Color online) Incoherent spectrum for (a) a saturating laser field,  $\Omega = \gamma_+/4 = 0.2625\gamma$ , and (b) a strong field  $\Omega = 3.5\gamma$ , with  $\gamma_d = 0.05\gamma$  and  $\gamma_a = 0.015\gamma$ . The solid (black) and dotted (red) curves are, respectively, the exact and approximate spectra, and the dashed (green) curve to the 2LA spectrum.

slightly smaller (bigger) in the saturating (strong) case than the exact one. Also, making  $\gamma_d = 0$  (hence  $q = 0$ ), the formula is exact for the 2LA spectrum [30]. The sharp peak, with amplitude proportional to  $C_2$ , Eq. (16b), is small for both weak and very strong driving.

The choice of values  $\gamma_d = 0.05\gamma$  and  $\gamma_a = 0.015\gamma$ , small enough to fulfill the limit (1), is such that the relation  $\gamma_d = 3.3\gamma_a$  closely optimizes the intensity of the sharp extra peak for any given Rabi frequency [5]. For simplicity, we use these values for all the remaining plots in this work.

### IV. THE SPECTRUM OF SQUEEZING

We turn now to the phase-dependent spectrum of the three-level atom and compare it to the well known case of the two-level atom [9, 31]. The so-called spectrum of squeezing is the spectrum of a quadrature of the emitted

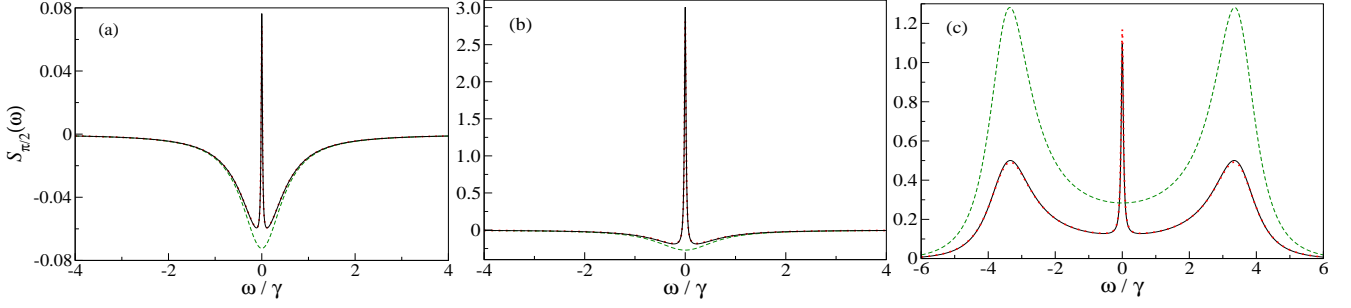


FIG. 3: (Color online) Spectra of the  $\phi = \pi/2$  quadrature for (a)  $\Omega = 0.1\gamma$ , (b)  $\Omega = 0.2625\gamma$ , (c)  $\Omega = 3.5\gamma$ . The other parameters are  $\gamma_d = 0.05\gamma$ ,  $\gamma_a = 0.015\gamma$ , and  $\eta = 1$ . The solid (black) and dotted (red) lines correspond to the exact and approximate 3LA spectra, respectively, and the dashed (green) lines are the 2LA spectra.

field,

$$\begin{aligned} S_\phi(\omega) &= 8\gamma_+\eta \int_0^\infty d\tau \cos \omega\tau \langle : \Delta\sigma_\phi(0)\Delta\sigma_\phi(\tau) : \rangle_{st} \\ &= 8\gamma_+\eta \int_0^\infty d\tau \cos \omega\tau \\ &\quad \times \text{Re} [e^{-i\phi} \langle \Delta\sigma_+(0)\Delta\sigma_\phi(\tau) \rangle_{st}] , \end{aligned} \quad (23)$$

where

$$\Delta\sigma_\phi = \frac{1}{2} (\Delta\sigma_- e^{i\phi} + \Delta\sigma_+ e^{-i\phi}) , \quad (24)$$

$\phi$  is the phase of the local oscillator in a balanced homodyne detector (BHD) setup (blocking the path to detector  $D_I$  in Fig. 1),  $\eta$  is a combined collection and detection

efficiency, and the dots  $::$  state that the operators must follow time and normal orderings. This is also an incoherent spectrum as it depends on the field fluctuations. In fact, the phase-dependent and the phase-independent spectra are related as [31],

$$S_{inc}(\omega) = \frac{1}{8\pi\alpha_{ee}\gamma_+\eta} [S_\phi(\omega) + S_{\phi+\pi/2}(\omega)] . \quad (25)$$

Adding the spectra for  $\phi = 0$  and  $\pi/2$  we recover Eq. (20).

Although the atom and laser parameters do not always allow for squeezing (negative values in the spectrum) we keep the moniker of spectrum of squeezing in order to distinguish this from the spectrum of Sec. VI.

Substituting Eqs. (15) and (16) into Eq. (23) the approximate spectra for the quadratures are:

$$S_0(\omega) = -8\gamma_+\eta C_1 \frac{\lambda_1}{\omega^2 + \lambda_1^2} , \quad (26)$$

$$\begin{aligned} S_{\pi/2}(\omega) &= 8\gamma_+\eta \left[ C_+ \frac{\lambda_+}{\omega^2 + \lambda_+^2} + C_- \frac{\lambda_-}{\omega^2 + \lambda_-^2} \right. \\ &\quad \left. - C_2 \frac{\lambda_2}{\omega^2 + \lambda_2^2} \right] . \end{aligned} \quad (27)$$

For  $\phi = 0$  the spectrum is only a single, positive (no squeezing) Lorentzian, just as for the 2LA, now of width  $\gamma_+$ . The positive, narrow extra peak appears only for  $\phi = \pi/2$  [last term of Eq. (27)]. Spectra of this quadrature are shown in Fig. 3 for several field strengths. For weak to moderate driving field there is squeezing except for a narrow band around the central frequency due to the extra peak. Rice and Carmichael [31] found that the weak field spectrum ( $Y^2 \ll 1$ ) has a line width smaller than  $\gamma/2$  due to the negative value of the Lorentzians

with  $\lambda_\pm$ , resulting in a squared Lorentzian [30]. In the 3LA the sharp peak destroys the subnatural line width, but squeezing sidebands remain. For strong fields, the spectrum consists of the sidebands of the Mollow triplet plus the extra peak.

An additional manifestation of shelving is the shrinking of the sidebands of the quadrature spectra compared to those of the 2LA. This is because the state  $|a\rangle$  takes an important fraction of the steady state population (actually  $\alpha_{aa} = q\alpha_{ee}$ ) for increasing Rabi frequency.

To further illustrate the difference among the spectra of quadratures, we plot in Fig. 4 the spectra of the correlations  $\langle \Delta\sigma_+(0)\Delta\sigma_\mp(\tau) \rangle_{st}$ . For  $S_0(\omega)$  the integrals are added, while for  $S_{\pi/2}(\omega)$  they are subtracted. Thus, the sharp peak resides only in the latter. The addition or subtraction cancels spectral components. The spectrum (20) contains only one of the integrals.

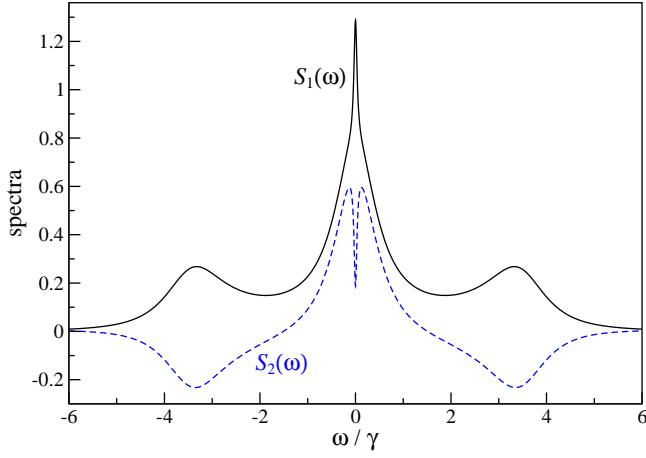


FIG. 4: (Color online) Spectra of the noise correlations  $\langle \Delta\sigma_+(0)\Delta\sigma_+(\tau) \rangle_{st}$  ( $S_1(\omega)$ —solid) and  $\langle \Delta\sigma_+(0)\Delta\sigma_-(\tau) \rangle_{st}$  ( $S_2(\omega)$ —dashed) for  $\Omega = 3.5\gamma$ ,  $\gamma_d = 0.05\gamma$ ,  $\gamma_a = 0.015\gamma$ , and  $\eta = 1$ .

### A. Variances and Integrated Spectra

An alternative approach to squeezing is the study of the variance or noise in a quadrature,

$$V_\phi = \langle : (\Delta\sigma_\phi)^2 : \rangle_{st} = \text{Re} [e^{-i\phi} \langle \Delta\sigma_+ \Delta\sigma_\phi \rangle_{st}] \quad (28)$$

or, equivalently, the integrated spectrum, related as  $\int_{-\infty}^{\infty} S_\phi(\omega) d\omega = 4\pi\gamma_+\eta V_\phi$ . A negative variance is a signature of squeezing in a quadrature. We have

$$V_0 = 2C_1 = \frac{1}{2} \frac{Y^2}{1 + Y^2 + (q/2)Y^2}, \quad (29a)$$

$$\begin{aligned} V_{\pi/2} &= 2[-C_+ - C_- + C_2] \\ &= \frac{Y^2/2}{(1 + Y^2)(1 + Y^2 + (q/2)Y^2)^2} \\ &\quad \times \left[ Y^4 \left( 1 + \frac{q}{2} \right) + \frac{q}{2} Y^2 - 1 \right]. \end{aligned} \quad (29b)$$

We plot the variances in Fig. 5.  $V_0$  is positive for any laser strength; there is no squeezing for  $\phi = 0$  but the total noise is smaller for the 3LA. For  $V_{\pi/2}$  both the interval of laser strength and amplitude for squeezing are notably reduced by the coupling to the long-lived state, and the Rabi frequency for the largest negative value is now very close to the saturating value  $\Omega = \gamma_+/4$ , which we use for several spectra.

The standard BHD technique depends on the finite detector efficiency  $\eta$ . This is a key obstacle to observe the weak squeezing of single atom resonance fluorescence. Only very recently the squeezing in the fluorescence of a single two-level quantum dot has been observed [20] with homodyne correlation measurements [11], which are independent of the detector efficiency. However, the measured variance had to be extracted from complementary measurements with different phases.

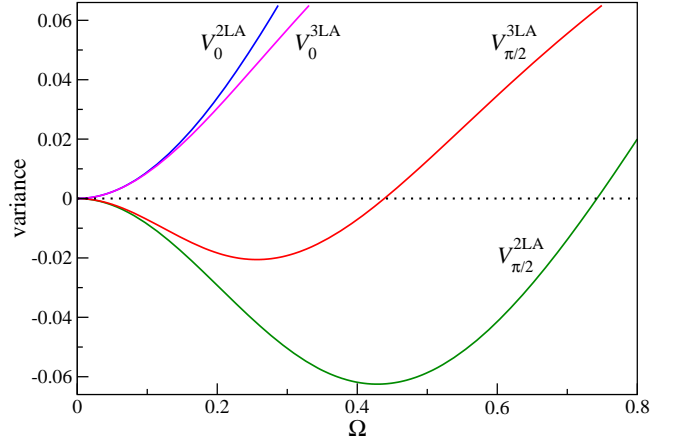


FIG. 5: (Color online) Variance of two and three-level atom resonance fluorescence for weak to moderately strong excitation, using Eqs. (29). Additional parameters for the 3LA are  $\gamma_d = 0.05\gamma$ ,  $\gamma_a = 0.015\gamma$ , and  $\eta = 1$ .

There is a subtle issue that also has to be addressed: Why is it that the quadrature variances are different? It seems natural to think that one features squeezing and the other doesn't. But, from the viewpoint of integrated spectra, one could expect this to be independent of the local oscillator phase. Thus, we reformulate the question: what spectrum is to be integrated that gives the same value for both quadratures?

Conditional homodyne detection (CHD) also solves the issue of finite detector efficiency, measuring an amplitude-intensity correlation, in this case without the need to extract the desired correlation from complementary measurements. CHD has been used to detect squeezing of a cavity QED source [14]. Additionally, CHD gives an answer to the missing term in the integrated spectra. We devote the next two Sections to a summary of CHD theory and its application to 3LA resonance fluorescence.

## V. CONDITIONAL HOMODYNE DETECTION

Figure 1 illustrates the setup for amplitude-intensity correlation by CHD. Its theory was first presented in [13] and its application to resonance fluorescence of a 2LA in [22, 23] and of a  $V$  three-level atom in [25–27]. Hence, here we show only its basic features. A quadrature of the field,  $E_\phi$ , is measured in balanced homodyne detection conditioned on the direct detection of a photon (intensity,  $I$ ) at detector  $D_I$ , i.e.,  $\langle I(0)E_\phi(\tau) \rangle_{st}$ . Here,  $E_\phi \propto \sqrt{\eta}\sigma_\phi$  and  $I \propto \eta\sigma_+\sigma_-$ . Upon normalization, the dependence of the correlation on the detector efficiency  $\eta$  is cancelled. Then

$$h_\phi(\tau) = \frac{\langle : \sigma_+(0)\sigma_-(0)\sigma_\phi(\tau) : \rangle_{st}}{\langle \sigma_+\sigma_- \rangle_{st} \langle \sigma_\phi \rangle_{st}}, \quad (30)$$

where it is assumed that the system is stationary,

$$\sigma_\phi = \frac{1}{2} (\sigma_- e^{i\phi} + \sigma_+ e^{-i\phi}), \quad (31)$$

is the dipole quadrature operator,  $\phi$  is the phase between the strong local oscillator and the driving field, and  $::$  indicates time and normal operator orderings. These orderings lead to different formulae for positive and negative time intervals and, in general, the correlations are asymmetric [13, 14, 24–28]. However, in the present case the correlation is symmetric, thus we only use the expression for positive intervals:

$$h_\phi(\tau) = \frac{\langle \sigma_+(0) \sigma_\phi(\tau) \sigma_-(0) \rangle_{st}}{\langle \sigma_+ \sigma_- \rangle_{st} \langle \sigma_\phi \rangle_{st}}. \quad (32)$$

When the laser excites the atom on-resonance, as is the case in this paper, the in-phase quadrature  $\langle \sigma_{\phi=0}(t) \rangle$  vanishes at all times, and likewise  $\langle \sigma_+(0) \sigma_0(\tau) \sigma_-(0) \rangle_{st} = 0$ . So, to obtain a finite measurement of this quadrature, it is necessary to add a coherent offset of amplitude  $E_{\text{off}}$  and phase  $\phi = 0$  to the dipole field before reaching the beam splitter [22]. This procedure, however, hides the non-classical character of the fluorescence, showing a monotonously decaying correlation:

$$h_0(\tau) = 1 + \frac{\alpha_{ee}}{\alpha_{ee} + E_{\text{off}}^2} e^{-\gamma_+ \tau/2}. \quad (33)$$

The  $\phi = \pi/2$  quadrature is more interesting. Substituting Eqs. (8a), (12) and (6) into Eq. (32) we obtain

$$h_{\pi/2}(\tau) = 1 - B_+ e^{\lambda_+ \tau} - B_- e^{\lambda_- \tau} + q \frac{Y^2/2}{1 + Y^2} e^{\lambda_2 \tau}, \quad (34)$$

where

$$B_\pm = \left( 1 + q \frac{Y^2/2}{1 + Y^2} \right) \left( \frac{1}{2} \pm \frac{1 - 2Y^2}{8\delta/\gamma_+} \right). \quad (35)$$

The coupling to the metastable level  $|a\rangle$  has visible consequences for both short and long times, making the CHD correlation amplitude larger than is the case for a 2LA, through the factor  $q = \gamma_d/\gamma_a$ . This excess amplitude decays slowly towards the unit value, which signals the decorrelation for long  $\tau$ , best noticed for large  $\Omega$ .

The CHD correlation can be written in terms of correlations of fluctuation operators, as is the case with the full incoherent and squeezing spectra. Splitting the dipole operators into a mean plus fluctuations, Eq. (13),  $h_\phi(\tau)$  is decomposed into a constant term plus two two-time correlations, one of second order and one of third order in the dipole fluctuation operators,

$$h_\phi(\tau) = 1 + h_\phi^{(2)}(\tau) + h_\phi^{(3)}(\tau), \quad (36a)$$

where

$$h_\phi^{(2)}(\tau) = \frac{2\text{Re}[\langle \sigma_- \rangle_{st} \langle \Delta \sigma_+(0) \Delta \sigma_\phi(\tau) \rangle_{st}]}{\langle \sigma_\phi \rangle_{st} \langle \sigma_+ \sigma_- \rangle_{st}}, \quad (36b)$$

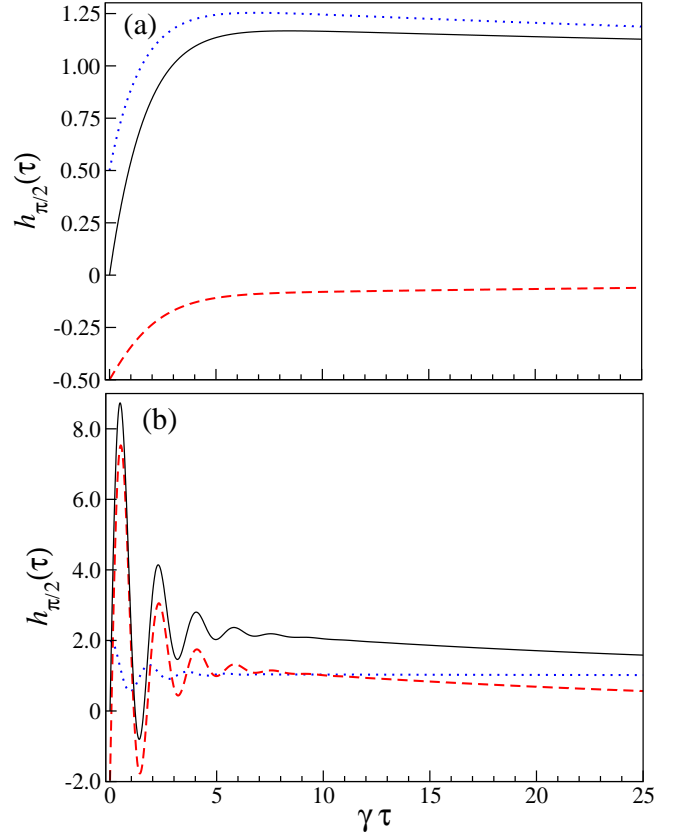


FIG. 6: (Color online) Amplitude-intensity correlation  $h_{\pi/2}(\tau)$  (solid-black), and its parts  $1 + h_{\pi/2}^{(2)}(\tau)$  (dotted-blue) and  $h_{\pi/2}^{(3)}(\tau)$  (dashed-red) for (a)  $\Omega = \gamma_+/4 = 0.2625\gamma$ , (b)  $\Omega = 3.5\gamma$ . The other parameters are  $\gamma_d = 0.05\gamma$  and  $\gamma_a = 0.015\gamma$ . Only the analytical results are plotted.

$$h_\phi^{(3)}(\tau) = \frac{\langle \Delta \sigma_+(0) \Delta \sigma_\phi(\tau) \Delta \sigma_-(0) \rangle_{st}}{\langle \sigma_\phi \rangle_{st} \langle \sigma_+ \sigma_- \rangle_{st}}. \quad (36c)$$

For  $\phi = 0$ , due to the need to add an offset, we are left with Eq. (33). For  $\phi = \pi/2$  we obtain the approximate expression:

$$h_{\pi/2}^{(2)}(\tau) = \frac{2}{\alpha_{ee}} [C_2 e^{\lambda_2 \tau} - C_+ e^{\lambda_+ \tau} - C_- e^{\lambda_- \tau}] \quad (37a)$$

$$h_{\pi/2}^{(3)}(\tau) = D_2 e^{\lambda_2 \tau} + D_+ e^{\lambda_+ \tau} + D_- e^{\lambda_- \tau}, \quad (37b)$$

where the coefficients  $D_2, D_\pm$  are too cumbersome to be reproduced here. In Fig. 6 we plot the analytical results, Eqs. (34) and (37a), which differ very little from the exact ones.

The vanishing of Eq. (36a) at  $\tau = 0$  has the same origin as the antibunching in the intensity correlations: when the atom is in the ground state upon a photon emission, both the dipole field and the intensity are zero, and they build up again when the atom reabsorbs light. For  $\phi = 0$



the effect is not seen due to the additional offset. So

$$\begin{aligned} h_{\pi/2}^{(2)}(0) &= \frac{\alpha_{ee} - 2|\alpha_+|^2}{\alpha_{ee}} \\ &= \frac{Y^2 + (q/2)Y^2 - 1}{1 + Y^2 + (q/2)Y^2}, \end{aligned} \quad (38a)$$

and

$$\begin{aligned} h_{\pi/2}^{(3)}(0) &= \frac{2(|\alpha_+|^2 - \alpha_{ee})}{\alpha_{ee}} = -2(2+q)\alpha_{ee} \\ &= -\frac{(2+q)Y^2}{1 + Y^2 + (q/2)Y^2}, \end{aligned} \quad (38b)$$

i.e., the initial size of the correlation is proportional to the mean population in the excited state. For  $\Omega \gg \gamma$ , the third order correlation has its largest (negative) initial value  $h_{\pi/2}^{(3)}(0) \rightarrow -2$ .

The third order term signals the deviation from Gaussian fluctuations as a consequence of the nonlinearity of the resonance fluorescence process for increasing laser intensity [22, 23]. As perhaps best noticed in the spectral domain, it is the enhanced sensitivity to nonlinearity that makes CHD to stand out over BHD and the spectrum of squeezing. We illustrate this in the next Section.

## VI. QUADRATURE SPECTRA FROM CHD

The spectrum measured from the amplitude-intensity correlation is given by

$$\mathcal{S}_\phi(\omega) = 4\gamma_+\alpha_{ee} \int_0^\infty d\tau \cos \omega\tau [h_\phi(\tau) - 1]. \quad (39)$$

Following the splitting of  $h_\phi(\tau)$ , Eq. (36a), the spectra of second and third order dipole fluctuations are

$$\mathcal{S}_\phi^{(2)}(\omega) = 4\gamma_+\alpha_{ee} \int_0^\infty d\tau \cos \omega\tau h_\phi^{(2)}(\tau), \quad (40a)$$

$$\mathcal{S}_\phi^{(3)}(\omega) = 4\gamma_+\alpha_{ee} \int_0^\infty d\tau \cos \omega\tau h_\phi^{(3)}(\tau), \quad (40b)$$

respectively. The splitting is not done by the measurement scheme but it can be calculated to provide valuable information about the system's fluctuations.

Initially, CHD was conceived to overcome the issue of imperfect detection and thus be able to measure squeezing of weak light sources [13, 14]. In the weak field limit

the spectrum of the amplitude-intensity correlation approaches the spectrum of squeezing if third order fluctuations can be neglected, i.e.,

$$S_\phi(\omega) = \eta \mathcal{S}_\phi^{(2)}(\omega) \approx \eta \mathcal{S}_\phi(\omega). \quad (41)$$

However, for not so weak fields, we find strong signatures of third order fluctuations in the spectra.

Using Eqs. (33) and (34) we obtain the approximate analytical spectra. For  $\phi = 0$ , we first make the replacement  $\alpha_{ee} \rightarrow \alpha_{ee} + E_{\text{off}}^2$  outside the integral, giving

$$\mathcal{S}_0(\omega) = \frac{4Y^2}{1 + Y^2 + (q/2)Y^2} \frac{\lambda_1^2}{\omega^2 + \lambda_1^2}, \quad (42)$$

which is independent of the offset. The spectrum of this quadrature is a simple Lorentzian of width  $\gamma_+$ . For  $\phi = \pi/2$  we have,

$$\begin{aligned} \mathcal{S}_{\pi/2}(\omega) &= \frac{\gamma_+ Y^2}{1 + Y^2 + (q/2)Y^2} \left\{ q \frac{Y^2}{1 + Y^2} \frac{\lambda_2}{\omega^2 + \lambda_2^2} \right. \\ &\quad \left. + B_+ \frac{\lambda_+}{\omega^2 + \lambda_+^2} + B_- \frac{\lambda_-}{\omega^2 + \lambda_-^2} \right\}. \end{aligned} \quad (43)$$

The second order spectra are

$$\mathcal{S}_0^{(2)}(\omega) = \mathcal{S}_0(\omega), \quad (44a)$$

$$\begin{aligned} \mathcal{S}_{\pi/2}^{(2)}(\omega) &= 8\gamma_+ \left[ C_+ \frac{\lambda_+}{\omega^2 + \lambda_+^2} + C_- \frac{\lambda_-}{\omega^2 + \lambda_-^2} \right. \\ &\quad \left. - C_2 \frac{\lambda_2}{\omega^2 + \lambda_2^2} \right]. \end{aligned} \quad (44b)$$

These are just the spectra of squeezing, Eqs. (26) and (27), without the detector efficiency factor. The third order spectrum  $\mathcal{S}_{\pi/2}^{(3)}(\omega) = \mathcal{S}_{\pi/2}(\omega) - \mathcal{S}_{\pi/2}^{(2)}(\omega)$  has a simple but cumbersome expression.

In Fig. 7 we plot the analytical results of the spectra of the amplitude-intensity correlation of the two- and three-level atom, Eq. (43). The difference from the exact results is very small. Note that for weak and saturating laser the sharp peak is smaller than in the spectra of squeezing, Fig. (3). This is because the third order sharp peak is negative in this excitation regime, as seen in the insets. Moreover, the full third order spectrum is negative, even for the 2LA, which enhances the negative squeezing peak and the non-classicality of the quadrature [22, 23].

---

In the strong excitation regime the third order spectrum leads to striking deviations among the CHD and squeezing spectra and among the 2LA and the 3LA. On the one hand, the sidebands become dispersive [22]. This comes out when  $\lambda_\pm$  become complex, that is, for  $\Omega > \gamma_+/4$ , but is visible only for strong enough excitation that the spectral components split. While the second order peaks are Lorentzians, the third order terms are dispersive and of comparable size for the 2LA or bigger for the 3LA. On the other hand are the large deviations in the size of spectra. The third order spectrum is much bigger in the 3LA than in the 2LA, not only for the sharp peak. They contribute most of the total CHD spectrum.



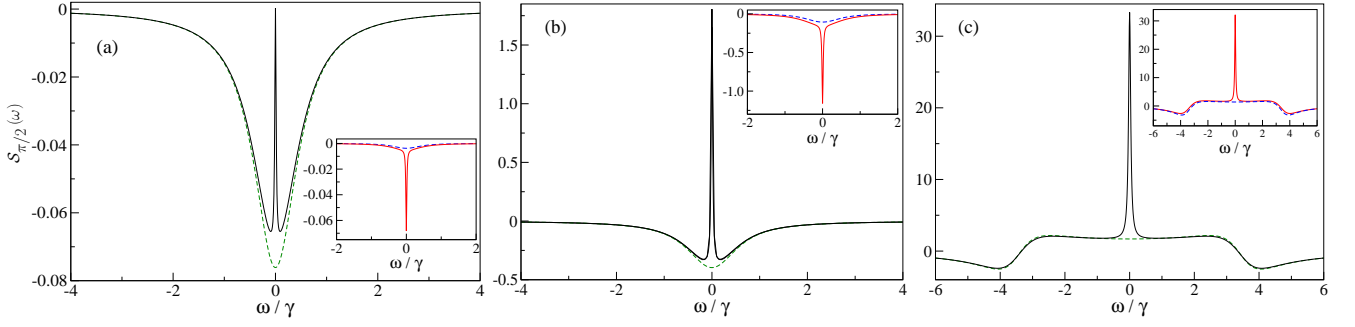


FIG. 7: (Color online) Spectra of the amplitude-intensity correlation for  $\phi = \pi/2$  of the three-level atom (solid-black) and two-level atom (dashed-green): (a) weak field  $\Omega = 0.1\gamma$ , (b) moderate field  $\Omega = \gamma_+/4 = 0.2625\gamma$ , and (c) strong field  $\Omega = 3.5\gamma$ . The insets show the third order spectra of the 3LA (solid-red) and 2LA (dashed-blue). The second order spectra are those of the spectrum of squeezing, Fig. 3. Only the analytical results are plotted.

The above effects can be explained as follows. The third order correlation of fluctuation operators gives a measure of the atom-laser nonlinearity, which grows with increasing laser intensity, and the deviation from Gaussian fluctuations of the fluorescence. Also, it should be mentioned that the dipole fluctuations of the driven transition are enhanced due to the coupling to the long-lived state  $|a\rangle$ , which is populated by the increased number of spontaneous emission events from the excited state, Eq. (6d). An early example of this effect in the three-level configuration of this paper is the reported large deviations in the photon statistics from those of a 2LA [32].

We recall that in the CHD spectrum the second and third order components cannot be measured separately. The former approaches the latter only in the weak driving regime. CHD goes beyond the concept of squeezing when studying phase-dependent fluctuations.

#### A. Variances and Integrated Spectra

Finally, we calculate the integrated spectra of the CHD quadratures:

$$\int_{-\infty}^{\infty} S_0(\omega) d\omega = 4\pi\gamma_+\alpha_{ee}, \quad (45a)$$

$$\int_{-\infty}^{\infty} S_{\pi/2}(\omega) d\omega = -4\pi\gamma_+\alpha_{ee} \left[ 1 + \frac{3qY^2}{4(1+Y^2)} \right]. \quad (45b)$$

Two points stand out. First, for a 2LA ( $q = 0$ ), the integrated spectra are equal, as found in [23]. This means that the total emitted noise is independent of the quadrature, as it should. This is made possible by the third order fluctuations, absent in the spectrum of squeezing, Sec. IV A. Second, for the 3LA, there is additional noise

due to the sharp extra peak which, as argued in [5], is intensity “transferred” from the elastic spectrum to the inelastic one, to the  $\phi = \pi/2$  quadrature to be specific as we show, due to the shelving effect.

## VII. CONCLUSIONS

We investigated ensemble-averaged phase-dependent fluctuations of the intermittent resonance fluorescence of a single three-level atom. We focused mainly on the spectrum of squeezing by balanced homodyne detection, and on the spectrum of the amplitude-intensity correlation of conditional homodyne detection. The shelving effect produces a sharp peak in the spectrum of the quadrature that features squeezing. In BHD this peak is positive, thus reducing the amount of squeezing. In CHD the sharp peak is negative in the weak to moderate excitation regime, thus enhancing the negative squeezing spectrum. This is because CHD is sensitive to third order dipole fluctuations that grow with atom-laser nonlinearity. Hence, for strong excitation, the spectra of BHD and CHD are very different. Additional insight is obtained calculating the variances or integrated spectra of quadratures. In BHD the variances are different, while in CHD they are equal, where the third order term provides the additional noise.

We considered only the case of exact atom-laser resonance. This allowed us to obtain very good approximate analytical solution of the master equation with a simple method, then used to construct analytical expressions for the various quantities of interest. Further insight into the incoherent spectrum and its link to the phase-dependent fluctuations could be established. Also, the on-resonance case allowed us to present the basic physical features in the most straightforward manner.

Conditional homodyne detection, with its sensitivity to third order field fluctuations, opens a new gate to study phase-dependent fluctuations beyond the realm of squeezing for highly nonlinear and non-Gaussian optical processes. On the other hand, the impressive advances in photon collection efficiencies by parabolic mirrors [10, 33] could complement CHD for atomic resonance fluorescence, its squeezing and its quantum fluctuations in general.

## Acknowledgments

HMCB thanks Prof. J. Récamier for hospitality at ICF-UNAM and PRODEP-UAEM for support. RRA thanks CONACYT for the scholarship No. 379732, and DGAPA-UNAM for support under project IN108413.

## Appendix A: Approximate Solutions

The approximate expectation values of the atomic operators are

$$\langle \sigma_{\mp}(t) \rangle = \mp i \frac{Y/\sqrt{2}}{1+Y^2} \left[ e^{\lambda_2 t} - e^{-3\gamma_+ t/4} \left( \cosh \delta t + \frac{3\gamma_+}{4\delta} \sinh \delta t \right) \right] \mp i\sqrt{2}Y \frac{\gamma_+}{4\delta} e^{-3\gamma_+ t/4} \sinh \delta t + \alpha_{\mp} (1 - e^{\lambda_2 t}) , \quad (\text{A1a})$$

$$\langle \sigma_{ee}(t) \rangle = \frac{Y^2/2}{1+Y^2} \left[ e^{\lambda_2 t} - e^{-3\gamma_+ t/4} \left( \cosh \delta t + \frac{3\gamma_+}{4\delta} \sinh \delta t \right) \right] + \frac{Y^2/2}{1+Y^2 + (q/2)Y^2} (1 - e^{\lambda_2 t}) , \quad (\text{A1b})$$

$$\langle \sigma_{gg}(t) \rangle = e^{\lambda_2 t} - \frac{Y^2/2}{1+Y^2} \left[ e^{\lambda_2 t} - e^{-3\gamma_+ t/4} \left( \cosh \delta t + \frac{3\gamma_+}{4\delta} \sinh \delta t \right) \right] + \frac{1 + (Y^2/2)}{1+Y^2 + (q/2)Y^2} (1 - e^{\lambda_2 t}) . \quad (\text{A1c})$$

We make several assumptions to give our results simple, albeit long, expressions: First, we neglect a term  $\gamma_d \Omega^2/2$  in the solutions in the Laplace space that reduce the problem to one similar to the 2LA case, with  $\gamma$  replaced by  $\gamma_+$ . Eigenvalues  $\lambda_{\pm}$  are thus identified. They give rise to the terms with the hyperbolic functions. Second, a constant term is multiplied by a factor  $e^{\lambda_2 t}$ . Finally, we add a term  $\langle \sigma_{jk} \rangle_{st} (1 - e^{\lambda_2 t})$ . Recall that for the case of a 2LA  $\lambda_2 = 0$  and  $\langle \sigma_{ee}(t) \rangle + \langle \sigma_{gg}(t) \rangle = 1$ . These *ad hoc* assumptions make the approximate solutions to approach the exact ones very well, as long as  $\gamma_d$  and  $\gamma_a$  are at least one order smaller than  $\gamma$ .

Similarly, we obtain

$$\begin{aligned} \langle \sigma_+(0) \sigma_{\mp}(\tau) \rangle_{st} &= \pm \frac{1}{2} \frac{Y^2}{(1+Y^2 + (q/2)Y^2)^2} + \frac{1}{4} \frac{Y^2}{1+Y^2 + (q/2)Y^2} e^{\lambda_1 \tau} \pm \frac{q}{4} \frac{Y^4}{(1+Y^2)(1+Y^2 + (q/2)Y^2)^2} e^{\lambda_2 \tau} \\ &\quad \mp \frac{1}{4} \frac{Y^2}{(1+Y^2)(1+Y^2 + (q/2)Y^2)} e^{-3\gamma_+ \tau/4} \left[ (1 - Y^2) \cosh \delta \tau \mp \frac{1 - 5Y^2}{4\delta/\gamma_+} \sinh \delta \tau \right] . \end{aligned} \quad (\text{A2})$$

## Appendix B: Equations of Motion

We solve sets of linear equations of motion for the expectation values of the atomic operators and for two-time correlations. The equations and the formal solutions can be written as

$$\frac{d}{dt} g(t) = \mathbf{M} g(t) , \quad (\text{B1})$$

$$g(t) = e^{\mathbf{M}t} g(0) , \quad (\text{B2})$$

where  $\mathbf{M}$  is the matrix (4b). In general, we solve these equations numerically. The initial conditions, though, are obtained exactly analytically, even off-resonance. For instance, defining  $\Delta \mathbf{s} \equiv (\Delta \sigma_-, \Delta \sigma_+, \Delta \sigma_{ee}, \Delta \sigma_{gg})^T$ , where  $\Delta \sigma_{jk} = \sigma_{jk} - \alpha_{jk}$  and  $\alpha_{jk} = \rho_{kj}^{st}$ ,  $\alpha_+ = \rho_{ge}^{st}$ ,  $\alpha_- = \rho_{eg}^{st}$ , the initial conditions of the second and third order correlations of the fluctuation operators are

$$\langle \Delta \sigma_+ \Delta \mathbf{s} \rangle_{st} = \begin{pmatrix} \alpha_{ee} - \alpha_+ \alpha_- \\ -\alpha_+^2 \\ -\alpha_+ \alpha_{ee} \\ \alpha_+ (1 - \alpha_{gg}) \end{pmatrix} = \frac{\Omega^2}{N^2} \begin{pmatrix} (2+q)\Omega^2 \\ \gamma_+^2 \\ -i\gamma_+ \Omega \\ i(1+q)\gamma_+ \Omega \end{pmatrix} , \quad (\text{B3})$$

$$\langle \Delta\sigma_+ \Delta s \Delta\sigma_- \rangle_{st} = \begin{pmatrix} 2\alpha_-(\alpha_+\alpha_- - \alpha_{ee}) \\ 2\alpha_+(\alpha_+\alpha_- - \alpha_{ee}) \\ \alpha_{ee}(2\alpha_+\alpha_- - \alpha_{ee}) \\ (\alpha_{gg} - 1)(2\alpha_+\alpha_- - \alpha_{ee}) \end{pmatrix} = \frac{\Omega^4}{N^3} \begin{pmatrix} i2(2+q)\gamma_+\Omega \\ -i2(2+q)\gamma_+\Omega \\ \gamma_+^2 - (2+q)\Omega^2 \\ (1+q)[\gamma_+^2 - (2+q)\Omega^2] \end{pmatrix}, \quad (\text{B4})$$

respectively, where we used the steady state values  $\alpha_{jk}$  of Eqs. (6) and  $N = (2+q)\Omega^2 + \gamma_+^2$ .

The calculations of spectra are more efficiently implemented using the formal solution  $g(\tau) = e^{\mathbf{M}\tau}g(0)$ , so the Fourier integral is formally solved as  $(i\omega\mathbf{1} - \mathbf{M})^{-1}g(0)$ , where  $\mathbf{1}$  is the  $4 \times 4$  identity matrix. One is saved potentially troublesome integrals where the upper limit is a long time of the order  $\gamma_d^{-1}$ .

- 
- [1] For a review see, e.g., M. B. Plenio and P. L. Knight, *Rev. Mod. Phys.* **70**, 101 (1997).
  - [2] F. D. Stefani, J. P. Hoogenboom, and E. Barkai, *Phys. Today* **62**, 34 (2009), February issue.
  - [3] G. C. Hegerfeldt and M. B. Plenio, *Phys. Rev. A* **52**, 3333 (1995).
  - [4] B. M. Garraway, M. S. Kim, and P. L. Knight, *Opt. Commun.* **117**, 550 (1995).
  - [5] J. Evers and Ch. H. Keitel, *Phys. Rev. A* **65**, 033813 (2002).
  - [6] V. Bühner and Chr. Tamm, *Phys. Rev. A* **61**, 061801 (2000).
  - [7] J. T. Höffges, H. W. Baldauf, W. Lange, and H. Walther, *J. Mod. Opt.* **44**, 1999 (1997).
  - [8] D. F. Walls and P. Zoller, *Phys. Rev. Lett.* **47**, 709 (1981).
  - [9] M. J. Collett, D. F. Walls, P. Zoller, *Opt. Commun.* **52**, 145 (1984).
  - [10] M. Sonderman and G. Leuchs, in *Engineering the Atom-Photon Interaction*, A. Predojevic and M. W. Mitchell, eds. (Springer-Verlag, Heidelberg, 2015).
  - [11] W. Vogel, *Phys. Rev. Lett.* **67**, 2450 (1991).
  - [12] W. Vogel, *Phys. Rev. A* **51**, 4160 (1995).
  - [13] H. J. Carmichael, H. M. Castro-Beltrán, G. T. Foster, and L. A. Orozco, *Phys. Rev. Lett.* **85**, 1855 (2000).
  - [14] G. T. Foster, L. A. Orozco, H. M. Castro-Beltrán, and H. J. Carmichael, *Phys. Rev. Lett.* **85**, 3149 (2000).
  - [15] H.-G. Hong, W. Seo, M. Lee, W. Choi, J.-H. Lee, and K. An, *Opt. Lett.* **31**, 3182 (2006).
  - [16] N. B. Grosse, Th. Symul, M. Stobińska, T. C. Ralph, and P. K. Lam, *Phys. Rev. Lett.* **98**, 153603 (2007).
  - [17] L. A. Krivitsky, U. L. Andersen, R. Dong, A. Huck, C. Wittmann, and G. Leuchs, *Phys. Rev. A* **79**, 033828 (2009).
  - [18] B. Kühn and W. Vogel, arXiv:1511.01723.
  - [19] H. J. Carmichael, *Phys. Rev. Lett.* **55**, 2790 (1985).
  - [20] C. H. H. Schulte, J. Hansom, A. E. Jones, C. Matthiesen, C. Le Gall, and M. Atatüre, *Nature* **525**, 222 (2015).
  - [21] S. Gerber, D. Rotter, L. Slodička, J. Eschner, H. J. Carmichael, and R. Blatt, *Phys. Rev. Lett.* **102**, 183601 (2009).
  - [22] H. M. Castro-Beltrán, *Opt. Commun.* **283**, 4680 (2008).
  - [23] H. M. Castro-Beltrán, L. Gutiérrez, and L. Horvath, *Appl. Math. Inf. Sci.* **9**, 2849 (2015).
  - [24] A. Denisov, H. M. Castro-Beltrán, and H. J. Carmichael, *Phys. Rev. Lett.* **88**, 243601 (2002).
  - [25] E. R. Marquina-Cruz and H. M. Castro-Beltrán, *Laser Phys.* **18**, 157 (2008).
  - [26] H. M. Castro-Beltrán, L. Gutiérrez, and E. R. Marquina-Cruz, in *Latin America Optics and Photonics*, Cancun, Mexico, 2014, OSA Technical Digest (Optical Society of America, 2014), paper LM4A.38.
  - [27] Q. Xu, E. Greplová, B. Julsgaard, and K. Mølmer, *Phys. Scripta* **90**, 128004 (2015).
  - [28] Q. Xu and K. Mølmer, *Phys. Rev. A* **92**, 033830 (2015).
  - [29] H. J. Carmichael, *Statistical Methods in Quantum Optics 1: Master Equations and Fokker-Planck Equations* (Springer-Verlag, Berlin, 2002).
  - [30] B. R. Mollow, *Phys. Rev.* **188**, 1969 (1969).
  - [31] P. R. Rice and H. J. Carmichael, *J. Opt. Soc. Am. B*, **5**, 1661 (1988).
  - [32] M. Merz and A. Schenzle, *Appl. Phys. B* **50**, 115 (1990).
  - [33] M. Stobińska, M. Sonderman, and G. Leuchs, *Opt. Commun.* **283**, 737 (2010).